Eur. Phys. J. D **24**, 311–314 (2003)
DOI: 10.1140/epjd/e2003-00179-4

THE EUROPEAN PHYSICAL JOURNAL D

Effect of epitaxial strain on the atomic structure of Pd clusters on MgO(100) substrate

A numerical simulation study

W. Vervisch, C. Mottet[a], and J. Goniakowski

CRMC2-CNRS, Campus de Luminy, case 913, 13288 Marseille Cedex 9, France

Received 10 September 2002
Published online 3 July 2003 –

Abstract. Morphology and atomic structure of supported Pd clusters on MgO(100) substrate are investigated theoretically using a mixed approach: a semi-empirical potential for the metal bonding within the cluster and a potential fitted to *ab initio* calculations for the metal-oxide interaction. We find that the clusters adopt a truncated pyramidal morphology in agreement with experimental results. The detailed study of the epitaxial relation as a function of cluster size shows the existence of a critical size around 3 nm where elastic strain due to the misfit between the substrate and the deposit is released by the introduction of interfacial dislocations.

PACS. 68.47.Jn Clusters on oxide surfaces – 61.46.+w Nanoscale materials: clusters, nanoparticles, nanotubes, and nanocrystals

1 Introduction

Free clusters have been widely studied theoretically [1,2] but most of experimental results and applications concern clusters in interaction with a support knowing that such interactions can give rise to a lot of different behaviors depending on the nature of the support and of the deposit [3]. For example, in the same experimental conditions, gold clusters can exhibit decahedral shape when deposited by low-energy cluster beam deposition on amorphous carbon whereas they always adopt truncated octahedral shape with the FCC symmetry when deposited in the same way on MgO single crystals [4]. Recent quantum-mechanical molecular dynamic simulations described cluster-surface interactions in the most reliable way but are still limited to very small clusters (about ten atoms) [5,6]. We propose here a mixed approach for treating metal cluster deposited on oxide surface in the nanometer size range, *i.e.* about 100 to many thousands of atoms. The energetic model used in molecular dynamic simulations consists in a classical tight-binding potential describing metal-metal bondings and an empirical potential fitted to *ab initio* calculations for metal-oxide bondings. Pd clusters supported by the MgO(100) surface is a model system both from theoretical and experimental point of view (see [7] and references therein).

[a] e-mail: mottet@crmc2.univ-mrs.fr

2 Model and method

Atomic structure determination for supported nanoscaled clusters requires efficient algorithms in order to find minimum energy structures for such complex systems (low symmetry and large number of atoms). We use quenched molecular dynamics with many different initial configurations and annealing procedure to prevent from being trapped in local minima. The interaction potential couples the well established second moment approximation (SMA) many body potential [8] in the tight binding formalism for metal-metal bonds and an analytical form fitted to *ab initio* calculations within the density-functional theory (DFT) based on full-potential linearized augmented-plane wave (FPLAPW) method [9] for metal-oxide interactions. The model has been detailed in a recent study [7]. It has to be noticed that the role played by oxygen vacancies on MgO(100) surface, although essential in the metal-oxide interaction for very small metallic clusters (1 to 10 atoms) [5,6,10], becomes less important for larger cluster sizes since the electron transfer induced by the surface color center remains localized to the close vicinity of the oxygen vacancy and the energy gain decreases with increasing Pd atoms coordination [10]. We have neglected it in the present study. An other assumption of the model consists in the neglection of atomic relaxations in the MgO oxide. This is not the case in general [11] but in that particular case, no MgO dilation is observed [12], and we checked by quantitative calculations of the energetic cost of the deformation the reliability of this assumption.

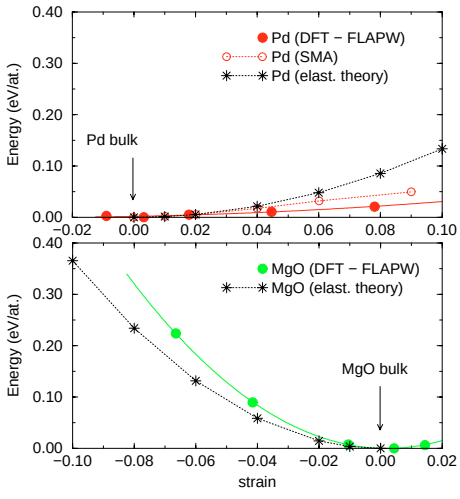

Fig. 1. Tetragonal deformation in Pd (upper graph) and MgO (lower graph) as a function of strain calculated using DFT – FLAPW, SMA (for Pd), and elastic theory calculations.

Table 1. Elastic constants (in GPa) [13].

	c_{11}	c_{12}	c_{44}	B	c'	ν
Pd	234	176	71	195	29	0.39
MgO	286	87	148	153	100	0.18

In Figure 1 we have plotted the energy relative to a tetragonal deformation of the Pd and MgO lattices when respectively dilated and contracted laterally, and free to relax perpendicularly. We compared the behavior of the metal and the oxide using DFT (or SMA) simulations with elastic theory prediction giving a square dependence of the energy *versus* strain:

$$E_{elast.} = \left(c_{11} + c_{12} - 2\frac{c_{12}^2}{c_{11}}\right) V_0 \epsilon^2 \qquad (1)$$

where c_{ij} are the elastic constants of the materials given in Table 1, V_0 is the atomic volume and ϵ the deformation. It costs clearly less energy to extend the metal than to contract the oxide, and this result is more pronounced in the DFT (or SMA) calculations than in the elastic theory which does not integrate the asymmetry of the interatomic potential coming from the fact that core-core repulsion is stronger than the attractive valence band term. This is not obvious comparing the bulk moduli (Tab. 1) of the two materials but can be deduced from their c' coefficient (for a tetragonal deformation at constant volume) or Poisson coefficient ν.

3 Cluster morphology: effect of the support

The study of the supported cluster morphology as a function of cluster size is performed starting from truncated octahedron as compared to free cluster morphology in the FCC structure [14]. We focus on FCC structure knowing that all the experimental results agree on the FCC

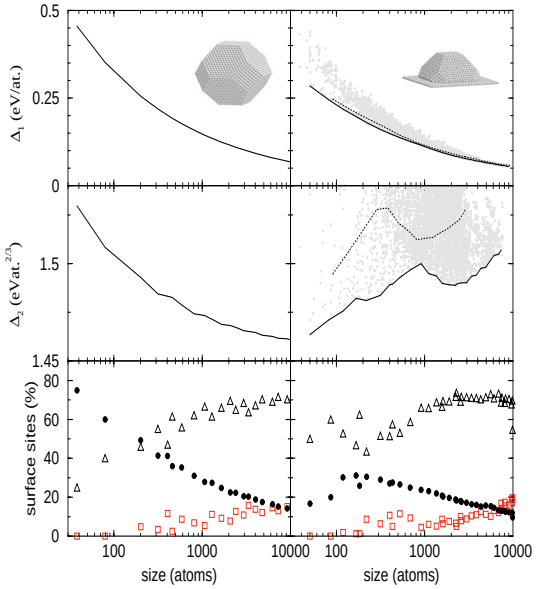

Fig. 2. Energetic quantities Δ_1 and Δ_2 plotted for free (left column) and supported (right column) clusters as a function of the clusters size. Dotted line curves represent perfect half pyramids (without truncation) and solid line curves correspond to the minimum energy ("equilibrium" shape). The bottom row displays the proportion of different type of surface sites: (111) facets (triangles symbols), (100) facets (squares) and edges (black points).

truncated octahedral structure for supported Pd clusters on MgO(100) substrate [15–17]. The results are shown in Figure 2. In the supported case, we have considered all the possible truncations (keeping the symmetry perpendicularly to the substrate) which explains the "cloud" of points in the second column of the figure. The optimized energies of clusters are defined taking as a reference the Pd bulk cohesion energy ϵ_B: $\Delta_1 = (E_{tot}(N) - \epsilon_B N)/N$ where $E_{tot}(N)$ is the total energy of a cluster of N atoms after atomic relaxation. It is important to notice that the plot of Δ_1 will necessarily show a decreasing tendency, converging slowly to zero, as the average energy of atoms in the cluster approaches the Pd bulk cohesive energy. This comes from the fact that as N increases, an increasing number of Pd atoms recover their bulk environment, and the relative contribution of under coordinated surface sites decreases. On the other hand, since the volume of a cluster is proportional to the number of atoms N, its surface area varies as $N^{2/3}$. Thus, the quantity Δ_2 defined as: $\Delta_2 = \Delta_1 N^{1/3}$ (in eV/at.$^{2/3}$) represents essentially the surface energy of the clusters, and is more sensitive to their relative stability. The curves are just a guide for the eyes that joins the points for given sizes. Growing cluster atom by atom would not drive to regular curve shape so there exist particular sizes for supported clusters presenting some enhancement of stability similar to magic number for free clusters. In the free case, Δ_2 tends monotonously to the average surface energy whereas in the supported case, the overall surface energy (free facets plus interface) follows an oscillating trends independently

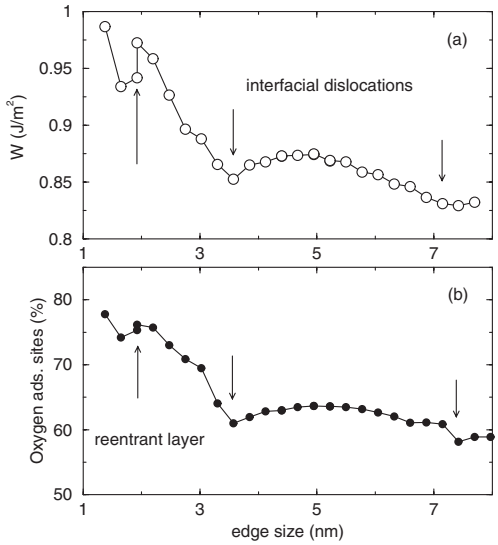

Fig. 3. Work of adhesion (a) and distribution of Pd atoms in the interfacial layer over the surface oxygen adsorption sites (b) as a function of cluster size for supported clusters in their equilibrium shape. The arrows indicate the introduction of the reentrant layer and interfacial dislocations.

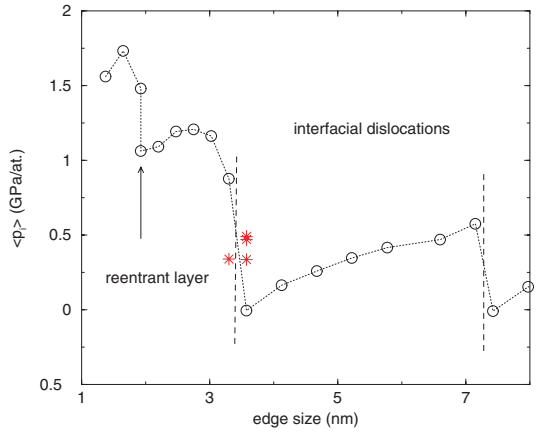

Fig. 4. Average atomic pressure per cluster and per atom as a function of cluster size for supported clusters in their equilibrium shape (circles) and for the alternative structure called "internal (111) faceting" (stars) which is illustrated in Figure 5a.

of the morphology. This is an important point that illustrates the cluster interaction with the substrate that will be discussed in the following.

Finally, we notice, looking at the bottom of Figure 2, that both kinds of clusters display roughly the same proportion of surface sites so that the supported clusters are roughly cut in their middle. The discrepancy observed at small sizes comes from the fact that we did not count the edge sites of supported clusters in contact with the substrate. As the supported clusters display one reentrant layer starting about 200 atoms in size (2 nm) [7], new edges sites appear in the same proportion as for free clusters. It seems then that the morphology of the supported clusters is not drastically affected by the support, as confirmed by the experimental evidence [15] and coherent with the non-reactive, weakly adhesive character of the Pd/MgO interface [18].

4 Epitaxial relation

The detailed study of the epitaxial relation as a function of clusters size [7] shows clearly two different regimes that are responsible of the non-monotonic behavior of the Δ_2 curves. We illustrate it by the analysis of the work of adhesion W, defined as the energy needed to separate the cluster from its support:

$$W = \frac{1}{S}\left(E_{free}^{\mathrm{Pd}} + E_{clean}^{\mathrm{MgO}} - E_{sup}^{\mathrm{Pd/MgO}}\right) \qquad (2)$$

where $E_{sup}^{\mathrm{Pd/MgO}}$ is the energy of a Pd cluster deposited on the MgO surface, and E_{free}^{Pd} and E_{clean}^{MgO} are respectively the energies of the free cluster and the clean MgO surface. We notice that Δ_2 (Fig. 2) and W (Fig. 3) display sensibly the same behavior (with an opposite sign).

At small sizes, the clusters undergo a tetragonal deformation [7] resulting from the pseudomorphic epitaxy. In that regime, 80% of the interface Pd atoms are on top of the preferential adsorption sites (oxygen sites) as illustrated in Figure 3b. As the lattice parameter of MgO is 8% larger than that of Pd, the Pd interatomic distances are dilated laterally. In order to keep a constant volume which is characteristic of metals, the vertical inter-atomic distances are contracted leading to the tetragonal deformation. The proportion of Pd atoms on top of oxygen sites decreases nearly monotonically when the cluster size increases (the first interruption corresponds to the introduction of the reentrant layer which contributes to improve the pseudomorphy). Around 3.5 nm, a transition related to the introduction of the first interface dislocation occurs, driving to a plastic regime where the elastic strain in Pd is partially released [11]. Such strain relief is well depicted by the evolution of the isostatic atomic pressure p_i equivalent to the trace of the stress tensor σ_{ij} on each atom i:

$$p_i = -\frac{1}{3}\sum_{i=1}^{3}\sigma_{ii} = -\frac{1}{3}\frac{\mathrm{d}E_i(r_{ij})}{\mathrm{d}r_{ij}}r_{ij} \qquad (3)$$

where E_i and r_{ij} are respectively the energy and interatomic distance related to the atom i and its neighbors j. The similarities of the curves in Figures 3 and 4 show how the interfacial energy is driven by the epitaxy-induced stress on the clusters.

In a local description of the epitaxial relation, the atomic pressure illustrated in Figure 5, shows that in the elastic regime, the Pd atoms are in tension in the neighborhood of the MgO whereas just after the introduction of the first interfacial dislocation, there is a local compressive stress corresponding to a Pd atomic row in coincidence with an Mg atomic row. As the size increases, such linear defects get organized in a network related to the lattice misfit, as observed for thicker film deposition [16].

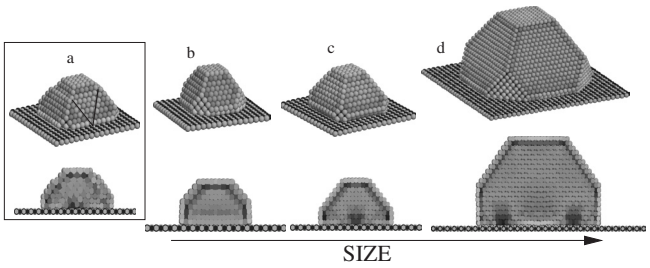

Fig. 5. Map of the atomic pressure across Pd clusters of different sizes. Upper graph represents the external morphology and lower graph represents a cutting view perpendicular to a ⟨100⟩ direction. The grey scale for Pd atoms represents the intensity of the pressure (light grey for tensile stress to dark grey for compressive stress). The MgO substrate displays black Mg atoms and white O atoms. (a) shows the alternative structure called "internal (111) faceting" whereas (b), (c) and (d) display clusters at different sizes.

In Figure 5a we plotted one alternative structure that is stable in a narrow size range near the transition from elastic to plastic regime. In order to minimize the local compressive stress, the first Pd layer at the interface separates in two pseudomorphic domains and the Pd row of the second plane is slightly lowered driving to a sliding according to the (111) dense planes. This new mechanism of strain relief has already been observed at metal hetero-interfaces with square symmetry in the case of Cu/Ni(100) by Müller *et al.* [19] who called it "internal (111) faceting".

Contrary to Müller and Kern [11] who show, in the framework of the elastic theory, a flattening of the shape for each dislocation entrance, we do not observe any morphologic change in the equilibrium cluster shape induced by the epitaxial strain. Nevertheless, we would like to mention that the atomic structure is inhomogeneously strained. Indeed, it has been shown (see Fig. 3 in Ref. [7]) that the epitaxial strain propagates in the cluster and vanishes beyond 5 or 6 interlayer spacings for large sizes but induces an inverse strain (lattice contraction) on the opposite layer (top facet) for smaller sizes. This has been predicted in elastic theory [20] and observed by scanning tunneling microscopy on the top of Ge islands epitaxially grown on Si(111) [21]. If it is confirmed on top of metallic clusters, such an atomic strain on cluster top facet could have a great impact on its catalytic properties since it has been shown both theoretically and experimentally that the adsorption energy of a molecule is modified by the lattice deformation [22,23].

5 Conclusions

For a model system *i.e.* Pd clusters in epitaxy with an MgO(100) surface, we have shown how the epitaxial strain induced by the substrate can influence the atomic and morphologic structure of the deposit. If the morphology of the supported clusters corresponds roughly to that of free FCC clusters cut in their middle, the local structure on the facets or at the interface is modified. At very small sizes, in the elastic regime, the interface and top facet of clusters are strained in an opposite way. At intermediate size, the epitaxy-induced stress is partially released by the entrance of interfacial dislocations or by an internal (111) faceting. At larger size, a dislocations network is established which mimics the structure of the infinite interface and the cluster surface sites are no more perturbed by the substrate.

The CRMC2 is associate to the Universities of Aix-Marseille II and III.

References

1. H. Haberland, *Clusters of Atoms and Molecules*, Springer Series in Chemical Physics (Springer Verlag, 1994), Vols. 1 and 2
2. W. Ekardt, *Metal Clusters*, Wiley Series in Theoretical Chemistry (John Wiley & Sons Ltd, Chichester, 1999)
3. K.H. Meiwes-Broer, *Metal Clusters at Surfaces*, Springer Series in Cluster Physics (Springer, Germany, 2000)
4. B. Pauwels, G. van Tendeloo, W. Bouwen, L.T. Kuhn, P. Lievens, H. Lei, M. Hou, Phys. Rev. B **62**, 10383 (2000)
5. A. Sanchez, S. Abbet, U. Heiz, W.D. Schneider, H. Häkkinen, R.N. Barnett, U. Landman, J. Phys. Chem. A **103**, 9573 (1999)
6. M. Moseler, H. Häkkinen, U. Landman, Phys. Rev. Lett. **89**, 176103 (2003)
7. W. Vervisch, C. Mottet, J. Goniakowski, Phys. Rev. B **65**, 245411 (2002)
8. V. Rosato, M. Guillopé, B. Legrand, Phil. Mag. A **59**, 321 (1984)
9. P. Blaha, K. Schwarz, J. Luitz, *WIEN97* (Vienna University of Technology, Vienna, 1997)
10. L. Giordano, J. Goniakowski, G. Pacchioni, Phys. Rev. B **64**, 075417 (2001)
11. P. Müller, R. Kern, Microsc. Microanal. Microstruct. **8**, 229 (1997); J. Cryst. Growth **193**, 257 (1998); Surf. Sci. **457**, 229 (2000)
12. S. Giorgio, C.R. Henry, C. Chapon, J.M. Penisson, J. Cryst. Growth **100**, 254 (1990)
13. G. Simmons, H. Wang, *Single crystal elastic constants and calculated aggregated properties* (MIT, Cambridge, 1971)
14. F. Baletto, R. Ferrando, A. Fortunelli, F. Montalenti, C. Mottet, J. Chem. Phys. **116**, 3856 (2002)
15. H. Graoui, S. Giorgio, C.R. Henry, Surf. Sci. **417**, 350 (1998); Phil. Mag. B **81**, 1649 (2001)
16. G. Renaud, A. Barbier, O. Robach, Phys. Rev. B **60**, 5872 (1999)
17. H. Fornander, L. Hulman, A.J. Birch, J.E. Sundgren, J. Cryst. Growth **186**, 189 (1998)
18. J. Goniakowski, Phys. Rev. B **59**, 11047 (1999)
19. B. Müller, B. Fischer, L. Nedelmann, A. Fricke, K. Kern, Phys. Rev. B **76**, 2358 (1996)
20. L.J. Gray, M.F. Chisholm, T. Kaplan, Appl. Phys. Lett. **66**, 1924 (1995)
21. S.K. Theiss, D.M. Chen, J.A. Golovchenko, Appl. Phys. Lett. **66**, 448 (1995)
22. M. Mavrikakis, B. Hammer, J.K. Norskov, Phys. Rev. Lett. **81**, 2819 (1998)
23. J.A. Rodriguez, D.W. Goodman, Science **257**, 897 (1992)